Hard x-ray photoelectron spectroscopy study of the electroforming in Ti/HfO2-based resistive switching structures

M. Sowinska, T. Bertaud, D. Walczyk, S. Thiess, M. A. Schubert et al.

Related Articles

Study of polarity effect in SiOx-based resistive switching memory
Appl. Phys. Lett. 101, 052111 (2012)

Ambipolar operation of hybrid SiC-carbon nanotube based thin film transistors for logic circuits applications
Appl. Phys. Lett. 101, 043121 (2012)

Non-volatile memory transistor based on Pt nanocrystals with negative differencial resistance
J. Appl. Phys. 112, 024319 (2012)

Resistive switching by migration of hydrogen ions
Appl. Phys. Lett. 101, 043507 (2012)

Controllable formation of resistive switching filaments by low-energy H+ irradiation in transition-metal oxides
Appl. Phys. Lett. 101, 043502 (2012)

Additional information on Appl. Phys. Lett.

Journal Homepage: http://apl.aip.org/

Journal Information: http://apl.aip.org/about/about_the_journal

Top downloads: http://apl.aip.org/features/most_downloaded

Information for Authors: http://apl.aip.org/authors

Hard x-ray photoelectron spectroscopy study of the electroforming in Ti/HfO₂-based resistive switching structures

M. Sowinska,[1,a)] T. Bertaud,[1] D. Walczyk,[1] S. Thiess,[2] M. A. Schubert,[1] M. Lukosius,[1] W. Drube,[2] Ch. Walczyk,[1] and T. Schroeder[1,3]

[1]*IHP, Im Technologiepark 25, 15236 Frankfurt (Oder), Germany*
[2]*Deutsches Elektronen-Synchrotron DESY, Notkestrasse 85, 22607 Hamburg, Germany*
[3]*Brandenburgische Technische Universität, Konrad-Zuse-Strasse 1, 03046 Cottbus, Germany*

The chemical and electronic modifications induced by the electroforming process on the Ti/HfO₂/TiN-based resistive switching devices were investigated by non-destructive hard x-ray photoelectron spectroscopy (HAXPES). The results indicate an increase of the titanium top electrode oxidation at the interface with HfO₂ after the electroforming process. Additionally, the binding energy values of the HAXPES peaks of the electroformed sample increased as compared to the as-prepared sample. The observed changes between both samples are attributed to the creation of *n*-type defects, such as oxygen vacancies, in the HfO₂ layer near the Ti interface during the electroforming process. © *2012 American Institute of Physics*. [http://dx.doi.org/10.1063/1.4728118]

A variety of different metal-insulator-metal (MIM) structures show reversible changes in the resistance upon applying bias voltages across the layers.[1–3] The application of current or voltage to an as-prepared device produces a significant change of its electronic conductivity.[4] An initial and irreversible process, called electroforming, is mostly required for obtaining a reversible and stable switching between a high (HRS) and a low (LRS) resistive state. The resistive switching (RS) effect is used to realize resistance change random access memory (RRAM) devices. Recently, there has been an increased interest in the use of transition metal oxides (TMO) as the insulator layer in the MIM stack for RRAM applications. Due to the compatibility with silicon complementary metal oxide semiconductor (Si CMOS) transistor technologies, Ti/HfO₂-based resistive switching devices are highly attractive,[5–8] even if the exact role of the Ti layer is not yet fully understood.[9]

Despite numerous efforts, the driving mechanism for the resistive switching effect of RRAM devices is still under debate.[1–3,10] For the TMO-based RRAMs, mainly two different mechanisms are considered. The first mechanism is attributed to the generation and rupture of metallic filaments,[11] e.g., by electromigration of metal atoms from the electrode with an applied electric field.[12] The second mechanism is based on the creation and annihilation of charged oxygen vacancies at the metal/oxide interface by redox processes.[4,13] Moreover, with applied bias, ionized oxygen vacancies can migrate across the MIM stack, creating conductive channels for the RS. Regrettably, oxygen vacancies are particularly unstable[14] and thus cannot be investigated by destructive techniques. Hard x-ray photoelectron spectroscopy (HAXPES) is a powerful synchrotron method to study deeply buried interfaces in a non-destructive way.[15] Although this technique has already shown its high potential to study the RS phenomenon in NiO-based RRAM device[14] and Cu/HfO₂-based RRAM device,[16] the electroforming step, as a prerequisite of the RS, is not fully explained, especially not for the HfO₂-based system, which is

gaining increased research interest as suitable candidate to enable future RRAM technologies.[17] Hence, in this work, we focus on understanding the chemical and electronic modifications that occur during this first electroforming process on CMOS-compatible Ti/HfO₂/TiN RRAM cells.[18]

For this purpose, a Ti/HfO₂/TiN thin film system was prepared on an 8 in. (001)-oriented Si wafer. A polycrystalline TiN bottom electrode was deposited by plasma assisted direct current magnetron sputtering of a titanium metal in the presence of a N₂/Ar gas mixture at room temperature (RT). An amorphous HfO₂ film was grown by atomic vapor deposition at 320 °C using a Hf(NMeEt)₄ precursor and oxygen as a reactive gas.[19] In the following step, a Ti top electrode was deposited by plasma vapor deposition at RT. Then, such prepared stack was characterized by x-ray reflection (XRR) and scanning transmission electron microscopy (STEM) with energy-dispersive x-ray spectroscopy (EDX) measurements. The results are presented in Fig. 1. From left to right are shown the high angle annular dark field STEM image with marked thicknesses of the layers obtained via XRR measurement (data not shown), and the Ti, O, Hf, and N EDX maps. Although the combined TEM-EDX study is a destructive technique, it allows deducing from the as-deposited sample qualitative information about the presence of a surface oxidation of the Ti top electrode and the existence of a Ti oxide interface layer between HfO₂ and the Ti metal electrode. Two samples of the same wafer, with a size of 1×1 mm², were subsequently diced. For the electrical measurements performed on one sample, a bottom electrode contact ($200 \times 200 \, \mu$m² in area as shown in the inset of Fig. 2(a)), was prepared by time of flight secondary ion mass spectroscopy depth profiling. With the bottom electrode set to ground potential, the electroforming process was performed under ambient conditions by applying a positive DC voltage sweep across the stack with a Keithley 4200 semiconductor characterization system. I-V characteristic of this initial electroforming process is presented in Fig. 2(a). After this electroforming process, the device presented a bipolar RS behavior by applying a voltage sweep from -3 to 6 V,

a)Author to whom correspondence should be addressed. Electronic mail: sowinska@ihp-microelectronics.com.
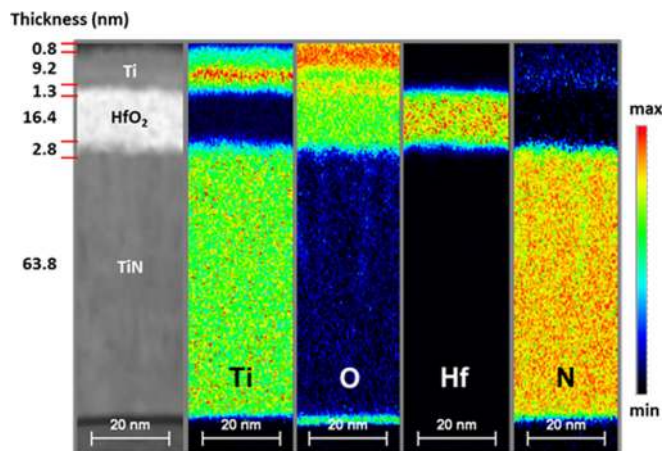
100, 233509-1

FIG. 1. High angle annular dark field STEM with EDX image of the as-prepared sample. These destructive techniques give qualitative information about pristine sample. Thicknesses of all layers were determined by XRR.

with a current compliance set at 80 mA, as shown in Fig. 2(b). Here, for the switching operation from LRS to HRS, a positive reset voltage was required, whereas a negative voltage was needed for the set operation from HRS to LRS. The two samples, called now as-prepared and electroformed, were then analyzed by HAXPES. The HAXPES measurements were carried out at the P09 beamline of the PETRA III storage ring at DESY (Hamburg).[20] Photoelectrons were excited at two photon energies, 5.5 and 7 keV, with a Si(311) double crystal monochromator in use. All HAXPES measurements were performed at a constant take-off angle of 90°. The SPECS Phoibos 225 HV electron analyser was mounted in polarisation direction of the x-ray beam. The photon energy was calibrated by means of the $4f_{7/2}$ signal from a metallic gold reference sample in electrical contact with the sample. The inelastic mean free paths were calculated using the TPP-2 M equation.[21] For the metallic Ti $2s$ line, they are equal to 8.6 and 10.4 nm for the two excitation energies of 5.5 and 7 keV, allowing the investigation of the Ti/HfO$_2$ interface. The Shirley background was removed from all recorded HAXPES spectra.

Our investigations revealed significant differences between the HAXPES spectra of as-prepared and electroformed samples. The two main observed phenomena are: a) chemical and b) electronic modifications.

The most prominent chemical changes occurred in the Ti spectra, and will be discussed first. Fig. 3 shows the Ti $2s$ HAXPES spectra of the as-prepared (top) and electroformed (bottom) samples collected at two excitation energies of 5.5 keV

(left) and 7 keV (right). All these spectra were modeled with three components attributed to metallic titanium (Ti), titanium suboxides (TiO$_x$), and titanium dioxide (TiO$_2$) with Gaussian-Lorentzian (for TiO$_x$ and TiO$_2$) and Doniach-Sunjic (for Ti) line shapes. The full width at half maximum of each component and the distance between the components were fixed for the HAXPES spectra simulation of both samples. Only the position and the intensity of the peak may thus change. The results of the simulations of the as-prepared sample spectra, presented in Figs. 3(a) and 3(b), also confirmed the two qualitative information given by the destructive techniques: (1) the titanium surface oxidation—attributed mainly to the existence of the TiO$_2$ component due to a higher intensity for both excitation energies than TiO$_x$, and (2) the existence of an interface layer composed of TiO$_x$ and TiO$_2$ between Ti and HfO$_2$—confirmed by the increase of both components by the increase of the sampling depth. Comparing the top with bottom spectra of Fig. 3, the electroforming process drastically changes the Ti $2s$ line shape. A decrease of the metallic Ti and an increase of the TiO$_2$ and TiO$_x$ peaks are clearly visible, confirming an enhanced Ti oxidation at the Ti/HfO$_2$ interface. To highlight the changes between the two investigated samples, the ratio between the metallic titanium to the total titanium oxides intensity (TiO$_x$ + TiO$_2$) was calculated and is further denoted as Ti/TiO$_y$. For the as-prepared sample, the Ti/TiO$_y$ ratio decreased from 1.5 ± 0.1 to 0.9 ± 0.1 when the excitation energy increased from 5.5 to 7 keV. The smaller Ti/TiO$_y$ ratio in case of the 7 keV excitation energy demonstrates that the HAXPES study is indeed sensitive to the oxidation of the Ti/HfO$_2$ interface, important for the switching mechanism. After electroforming, an enhanced Ti/HfO$_2$ interface oxidation is observed, resulting in an even smaller Ti/TiO$_y$ ratio of 0.6 ± 0.1 at 7 keV. Interestingly, only minor differences in the Ti $2s$ peak shape were observed for the electroformed sample spectra recorded at the two different photon energies: for both cases, the Ti/TiO$_y$ ratio is equal to 0.6 ± 0.1. This can indicate a creation of a more homogeneous system during the electroforming step with an oxygen migration from HfO$_2$ into the Ti layer. In addition, it is also noticed that the simulation of the Ti $2p$ HAXPES spectra (not shown) corroborates the same results presented here with the less complex Ti $2s$ line. Due to the higher sensitivity of the 7 keV excitation energy to the important Ti/HfO$_2$ interface, the next HAXPES results on other photoelectron lines will be only presented at this energy.

Second, besides the chemical changes, electronic modifications appeared also in the HAXPES spectra via changes in the peak positions. After the electroforming process, the HAXPES peak positions (marked with vertical dashed-
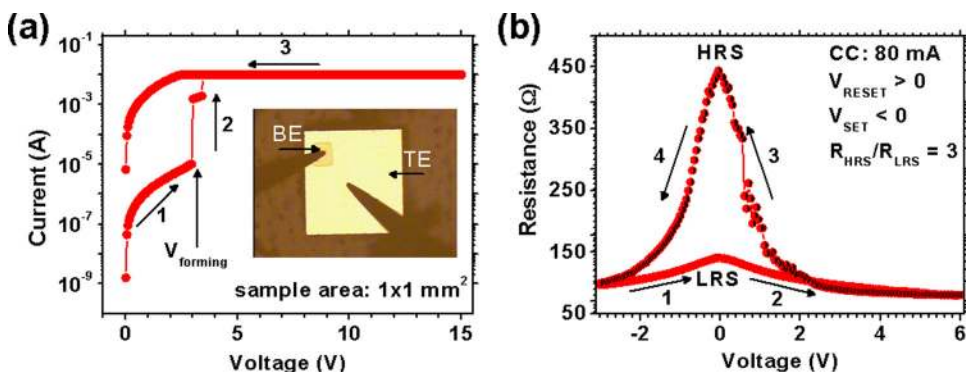

FIG. 2. (a) I-V characteristic of the initial electroforming process applied to the as-prepared stack (sweep rate 0.05 V/s). Inset shows a top view of the sample with the bottom (BE) and top (TE) electrode contacts. (b) R-V characteristic of the electroformed sample presenting a bipolar resistive switching.
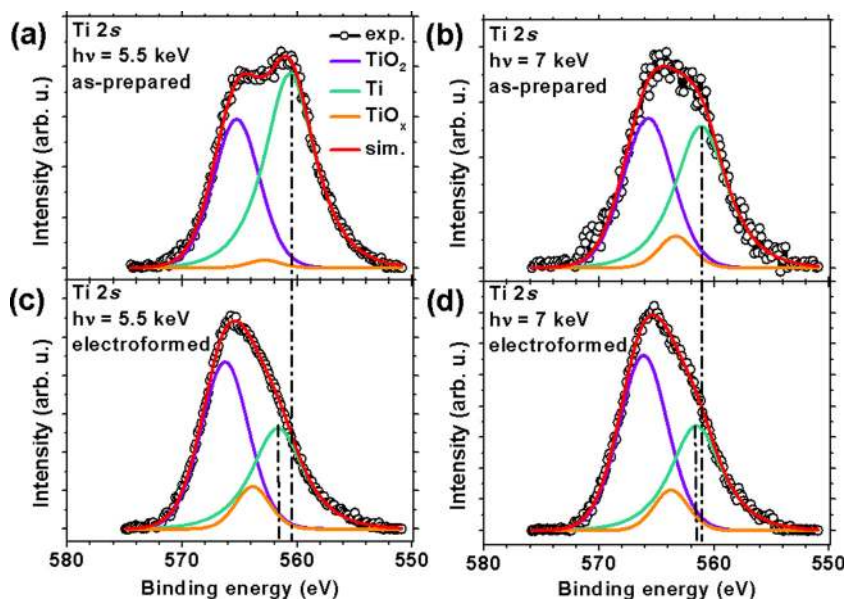
FIG. 3. Ti 2*s* HAXPES spectra of the as-prepared (top) and electroformed (bottom) samples taken with 5.5 keV (left) and 7 keV (right) excitation energy. All spectra are normalized and modeled with three components. Dashed-dotted lines highlight the changes in the peak position between the as-prepared and electroformed samples.

dotted lines in Figs. 3, 4(a), and 4(b)) are shifted towards larger binding energy (BE) with respect to the as-prepared sample. Table I summarizes the values of the difference (ΔBE) in the metallic Ti 2*s*, Hf 4$d_{5/2}$, and O 1*s* peak positions of the two investigated samples before and after electroforming. Since the peak shift values upon electroforming for Hf 4*d* (0.8 eV) and O 1*s* (0.7 eV) are almost the same and higher than that for Ti 2*s* (0.4 eV), we assume that the oxygen signal arises mainly from HfO$_2$ sample region. Moreover, because ΔBE values for these three components are different, a sample charging during measurement or an interface dipole creation can be excluded as a reason of these shifts.[22]

Finally, in order to highlight the chemical changes in the Hf 4*d* and O 1*s* XPS peak shapes in the Figs. 4(c) and 4(d), the energy shift after electroforming was corrected. It is seen that no clear chemical changes are visible for the Hf 4*d* spectra. However, a small change appears in the O 1*s*, high-

lighted in the inset of Fig. 4(d). For the as-prepared sample, a small subpeak located around 532.5 eV decreases after the electroforming step. We speculate that this subpeak could be attributed to the more covalently bonded, probably defect-related oxygen entities in the HfO$_2$ film. It is noted that such species were previously reported in the literature and termed "non-lattice oxygen."[23] Such defect-related oxygen entities are prone to move in the oxide layer, with lower activation energy during electroforming.[24] Hence, they leave oxygen vacancies in the HfO$_2$ layer behind.

Based on these results, we present in Fig. 5 the possible chemical (top) and electronic (bottom) modifications in the Ti/HfO$_2$/TiN MIM stack between the as-prepared (left) and electroformed (right) samples. The applied positive voltage to the MIM stack results in an oxygen migration towards the top electrode enhancing the Ti/HfO$_2$ interface oxidation and thus increasing the TiO$_y$ interface layer thickness between Ti and HfO$_2$. Removed oxygen atoms from the HfO$_2$ layer
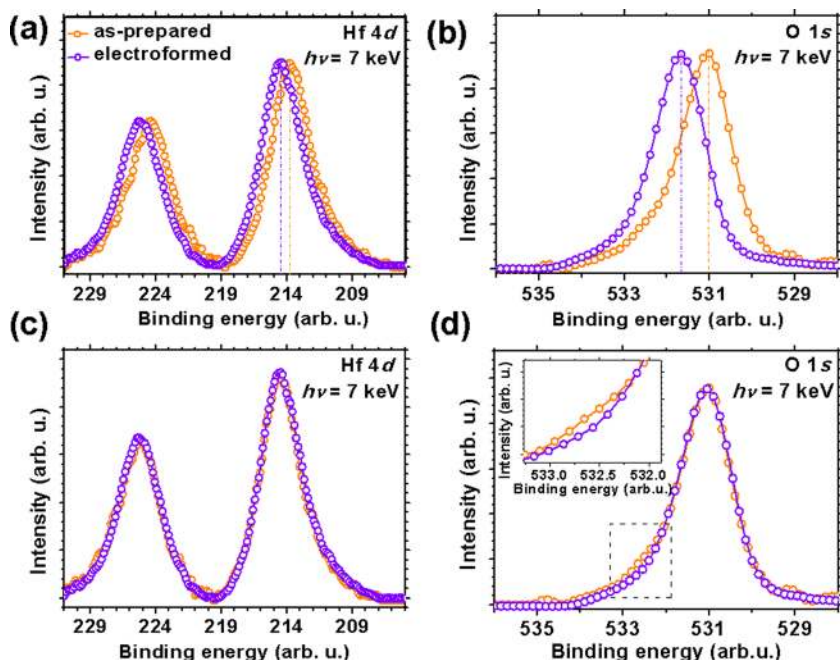

FIG. 4. Normalized and smoothed Hf 4*d* [(a) and (c)] and O 1*s* [(b) and (d)] HAXPES spectra of the as-prepared and electroformed samples recorded at excitation energy of 7 keV. [(a) and (b)] Dashed-dotted lines highlight the shifts in the peak position (note that the x-axis scales for Hf and O are different). The values of these shifts are presented in Table I. [(c) and (d)] Energy shift after electroforming was corrected in order to compare changes in the peak shape: no changes in the Hf 4*d* but a small change in the O 1*s* spectra were observed. The latter is highlighted in the inset of (d), which zooms on the region corresponding to the covalently bonded, probably defect-related oxygen entities in the HfO$_2$ film.

TABLE I. Experimental peak shifts ($\Delta BE = BE_{electroformed} - BE_{as\text{-}prepared}$) between the electroformed and as-prepared samples, for metallic Ti $2s$, Hf $4d_{5/2}$, and O $1s$ lines, recorded with excitation energy of 7 keV.

	Peak		
	Ti $2s$	Hf $4d_{5/2}$	O $1s$
$\Delta BE \pm 0.05$ (eV)	0.4	0.8	0.7

leave oxygen vacancies behind, as discussed hereafter. The formation of oxygen vacancies known as stable *n*-type defects in HfO_2 (Refs. 23 and 25) was also predicted by theory.[26,27] Besides, as previously shown in Fig. 2, the investigated sample presents a bipolar RS behavior with negative set and positive reset voltage polarities. The same switching polarities are found in *n*-type doped complex perovskite dielectric-based RRAMs.[3,4,28,29] Then, as discussed by other groups,[30,31] we propose that the observed XPS peak shifts are a consequence of an increase of the downward band bending due to an increase of *n*-type oxygen vacancy dopants at the Ti/HfO_2 interface. To illustrate this point, the band diagrams of the as-prepared and electroformed Ti/HfO_2/TiN stack at equilibrium[32] (i.e., all the Fermi position are equal) are drawn in Fig. 5. Knowing the higher work function of the TiN bottom electrode ($\Phi^{TiN} = 4.7$ eV) (Ref. 33) compared to the Ti top electrode ($\Phi^{Ti} = 4.2$ eV),[26] and that the barrier height for top injection is lower than the barrier height for bottom injection,[34] we propose in Fig. 5 on the bottom left, the band diagram of the as-prepared sample with a downward band bending towards the Ti top electrode.[32] Moving on to the electroformed sample, the downward band

bending increases due to an increase of the *n*-type dopants concentration (oxygen vacancies) at the interface. As a consequence, the binding energy (BE)—here exemplified for valence band (VB) maximum photoelectrons by the energy difference between E_F and the VB maximum—increases and the barrier height (Φ_b) decreases. This reduced barrier height explains the observed higher conductivity of the electroformed sample.

In conclusion, the first electroforming process on Ti/HfO_2/TiN-based RRAM cells was investigated by non-destructive HAXPES method, which has underlined both chemical and electronic modifications at the Ti/HfO_2 interface. This process prepares the RRAM material to enable specific RS mechanism by generating charges in the HfO_2 insulator that have certain mobility and that can be reversibly driven around by applied electric fields of opposite polarity. A detailed analysis of these results indicates an increase of the Ti oxidation at the Ti/HfO_2 interface and concomitant creation of oxygen vacancies in the HfO_2 dielectric layer during the electroforming process. The observed peak shifts towards larger BE are a consequence of a downward band bending at the interface which confirms the *n*-type doping of the insulator. Future HAXPES investigations by our group will thus focus on unveiling the physics of the switching mechanism, namely by *in-situ* switching experiments to dynamically monitor the material changes as a function of electrical stimuli of one and the same sample to exclude variation across the wafer.
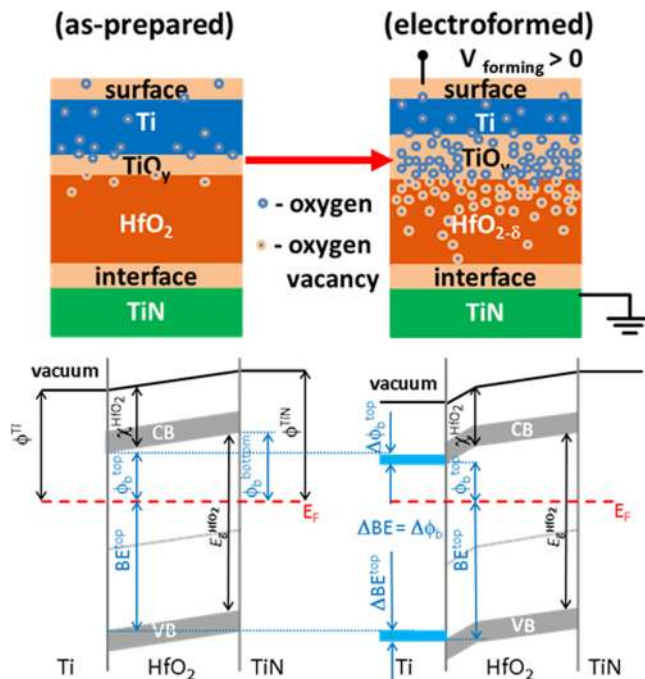
FIG. 5. Proposed chemical (top) and electronic (bottom) modifications of the Ti/HfO_2 interface between the as-prepared (left) and electroformed (right) samples. An increase of the *n*-type oxygen vacancy (Vö) defects at the Ti/HfO_2 interface during the electroforming process increases the downward band bending, thereby increasing the sample conductivity. (Φ_b—barrier height, Φ—work function, BE—binding energy, E_g—band gap, CB—conduction band, VB—valence band, χ—electron affinity).

[1]J. Wu, J. Cao, W.-Q. Han, A. Janotti, and H.-C. Kim, *Functional Metal Oxide Nanostructures* (Springer, Berlin, 2012).
[2]S. Ramanathan, *Thin Film Metal Oxides: Fundamentals and Applications in Electronics and Energy* (Springer, Berlin, 2010).
[3]A. Sawa, Mater. Today **11**, 28 (2008).
[4]J. J. Yang, F. Miao, M. D Pickett, D. A. A. Ohlberg, D. R Stewart, C. N. Lau, and R S Williams, Nanotechnology **20**, 215201 (2009).
[5]P.-S. Chen, H.-Y. Lee, Y.-S. Chen, P.-Y. Gu, F. Chen, and M.-J. Tsai, Electrochem. Solid-State Lett. **13**, H423 (2010).
[6]Y.-S. Chen, H.-Y. Lee, P.-S. Chen, T.-Y. Wu, C.-C. Wang, P.-J. T. Chen, F. M.-J. Tsai, and C. Lien, IEEE Electron Device Lett. **31**, 1473 (2010).
[7]Ch. Walczyk, Ch. Wenger, D. Walczyk, M. Lukosius, I. Costina, M. Fraschke, J. Dabrowski, A. Fox, D. Wolansky, S. Thiess, E. Miranda, B. Tillack, and T. Schroeder, J. Vac. Sci. Technol. B **29**, 01AD02 (2011).
[8]Ch. Walczyk, D. Walczyk, T. Schroeder, T. Bertaud, M. Sowinska, M. Lukosius, M. Fraschke, D. Wolansky, B. Tillack, E. Miranda, and Ch. Wenger, IEEE Trans. Electron Devices **58**, 3124 (2011).
[9]T. Bertaud, D. Walczyk, Ch. Walczyk, S. Kubotsch, M. Sowinska, T. Schroeder, Ch. Wenger, C. Vallée, P. Gonon, C. Mannequin, V. Jousseaume, and H. Grampeix, Thin Solid Films **520**, 4551 (2012).
[10]R. Waser, R. Dittmann, G. Staikov, and K. Szot, Adv. Mater. **21**, 2632 (2009).
[11]R. Waser and M. Aono, Nature Mater. **6**, 833 (2007).
[12]J. F. Gibbons and W. E. Beadle, Solid-State Electron **7**, 785 (1964).
[13]B. P. Andreasson, M. Janousch, U. Staub, G. I. Meijer, A. Ramar, J. Krbanjevic, and R. Schaeublin, J. Phys.: Conf. Ser. **190**, 012074 (2009).

[14]P. Calka, E. Martinez, D. Lafond, S. Minoret, S. Tirano, B. Detlefs, J. Roy, J. Zegenhagen, and C. Guedj, J. Appl. Phys. **109**, 124507 (2011).

[15]S. Thiess, C. Kunz, B. C. C. Cowie, T.-L. Lee, M. Renier, and J. Zegenhagen, Solid State Commun. **132**, 589 (2004).

[16]T. Nagata, M. Haemori, Y. Yamashita, H. Yoshikawa, Y. Iwashita, K. Kobayashi, and T. Chikyow, Appl. Phys. Lett. **99**, 223517 (2011).

[17]S.-S. Sheu, M.-F. Chang, K.-F. Lin, C.-W. Wu, Y.-S. Chen, P.-F. Chiu, C.-C. Kuo, Y.-S. Yang, P.-C. Chiang, W.-P. Lin, C.-H. Lin, H.-Y. Lee, P.-Y. Gu, S.-M. Wang, F. Chen, K.-L. Su, C.-H. Lien, K.-H. Cheng, H.-T. Wu, T.-K. Ku, M.-J. Kao and M.-J. Tsai, Tech. Dig. –Int. Solid-State Circuits Conference, **2011**, pp. 200–201.

[18]D. Walczyk, Ch. Walczyk, T. Schroeder, T. Bertaud, M. Sowinska, M. Lukosius, M. Fraschke, B. Tillack, and Ch. Wenger, Microelectron. Eng. **88**, 1133 (2011).

[19]Ch. Wenger, M. Lukosius, H.-J. Müssig, G. Ruhl, S. Pasko, and Ch. Lohe, J. Vac. Sci. Technol. B **27**, 286 (2009).

[20]A. Gloskovskii, G. Stryganyuk, G. H. Fecher, C. Felser, S. Thiess, H. Schulz-Ritter, W. Drube, G. Berner, M. Sing, and R. Claessen, J. Electron Spectrosc. Relat. Phenom. **185**, 47 (2012).

[21]S. Tanuma, C. J. Powell, and D. R. Penn, Surf. Interface Anal. **21**, 165 (1994).

[22]C. C. Fulton, G. Lucovsky, and R. J. Nemanich, Appl. Phys. Lett. **84**, 580 (2004).

[23]M. K. Yang, J.-W. Park, T. K. Ko, and J.-K. Lee, Appl. Phys. Lett. **95**, 042105 (2009).

[24]S. Yu, Y. Y. Chen, X. Guan, H.-S. P. Wong, and J. A. Kittl, Appl. Phys. Lett. **100**, 043507 (2012).

[25]D.-Y. Cho, J. M. Lee, S.-J. Oh, H. Jang, J.-Y. Kim, J.-H. Park, and A. Tanaka, Phys. Rev. B **76**, 165411 (2007).

[26]J. Robertson, O. Sharia, and A. A. Demkov, Appl. Phys. Lett. **91**, 132912 (2007).

[27]P. Brouqvist and A. Pasquarello, Appl. Phys. Lett. **89**, 262904 (2006).

[28]T. Fujii, M. Kawasaki, A. Sawa, H. Akoh, Y. Kawazoe, and Y. Tokura, Appl. Phys. Lett. **86**, 012107 (2005).

[29]T. Fujii, M. Kawasaki, A. Sawa, Y. Kawazoe, H. Akoh, and Y. Tokura, Phys. Rev. B **75**, 165101 (2007).

[30]Y. Lebedinskii, A. Zenkievich, and E. P. Gusev, J. Appl. Phys. **101**, 074504 (2007).

[31]C. L. Hinkle, R. V. Galatage, R. A. Chapman, E. M. Vogel, H. N. Alshareef, C. Freeman, E. Wimmer, H. Niimi, A. Li-Fatou, J. B. Shaw, and J. J. Chambers, Appl. Phys. Lett. **96**, 103502 (2010).

[32]S. M. Sze and K. K. Ng, *Physics of Semiconductor Devices* (John Wiley & Sons, Hoboken, 2006), pp. 22–27.

[33]Ch. Walczyk, Ch. Wenger, R. Sohal, M. Lukosius, A. Fox, J. Dąbrowski, D. Wolansky, B. Tillack, H.-J. Müssig, and T. Schroeder, J. Appl. Phys. **105**, 114103 (2009).

[34]V. Afanas'ev, private communication (2011).